Imidazole and 1,2,4-Triazole-based Derivatives Gifted with Antitubercular Activity: Cytotoxicity and Computational Assessment

Daniele Zampieri[a,*], Francesca Cateni[a], Mariarosa Moneghini[a], Marina Zacchigna[a], Erik Laurini[b], Domenico Marson[b], Alessandro De Logu[c], Adriana Sanna[c] and Maria G. Mamolo[a]

[a]Department of Chemistry and Pharmaceutical Sciences, P.le Europa 1, University of Trieste, 34127 Trieste, Italy; [b]Molecular Simulation Engineering (MOSE) Laboratory, DEA, Via Valerio,10, University of Trieste, 34127 Trieste, Italy; [c]Department of Life and Enviromental Sciences, Via Porcell, 4, University of Cagliari, 09124 Cagliari, Italy

Abstract: Background: *Mycobacterium Tuberculosis* (Mtb) is the causative pathogen of Tuberculosis (TB) and outbreaks are more common among immunosuppressed persons infected with HIV. The current treatment regimens are lengthy and toxic, yet the therapy has remained unchanged for many decades, so there is a need to find new structures with selective mechanism of action. Moreover, the increased incidence of severe disseminated infections produced by undiagnosed Multidrug-resistant (MDR), worsen clinical treatment and contribute the spread of the disease.

Objective: The aim of our study was to evaluate the potential of imidazole and triazole moieties for antimycobacterial activity, by synthesizing some 1-(1-(aryl)-2-(2,6-dichlorophenyl)hydrazono)ethyl-1*H*-imidazole and 1*H*-1,2,4-triazole derivatives **2a-l**.

Methods: The title compounds were obtained *via* classical organic synthesis. The antimicrobial activity was evaluated using the method of microdilution and the cytotoxicity assay was performed by MTT method.

Results: The results indicated that the presence of both the imidazole ring and that of the 2,6-dichlorosubstituted phenyl moiety, is more relevant for inhibitory activity against Mtb than the triazole nucleus and the unsubstituted phenyl ring. Among the series, *(E)*-1-(2-(5-chlorothiophen-2-yl)-2-(2-(2,6-dichlorophenyl)hydrazono)ethyl)-1*H*-imidazole derivative **2f** and *(Z)*-1-(2-([1,1'-biphenyl]-4-yl)-2-(2-(2,6-dichlorophenyl)hydrazono)ethyl]-1*H*-imidazole derivatives **2e** exhibited a promising antimycobacterial property and the latter also displayed a safe cytotoxic profile.

Conclusion: The synthesized compounds were studied for their antitubercular activity. Among the series, the compounds **2e** and **2f** appeared to be the most promising agents and, according to the docking assessment, the compounds could be CYP51 inhibitors. These evidences could be useful for the future development of new antimycobacterial derivatives targeting CYP51 with more specificity for the mycobacterial cell enzyme.

1. INTRODUCTION

Although the number of Tuberculosis (TB) deaths fell by 22% between 2000 and 2015, TB remained one of the top 10 causes of death worldwide in 2016 with 1.4 million deaths estimated among HIV-negative people and 10.4 million new TB cases worldwide [1].

Mycobacterium Tuberculosis (Mtb) is the causative pathogen of the TB and outbreaks are more common among immunosuppressed persons infected with HIV. The current treatment regimens are lengthy and toxic, yet the therapy has remained unchanged for many decades, so there is a need to find new structures with selective mechanism of action. Moreover, the increased incidence of severe disseminated infections produced by undiagnosed Multi-Drug-Resistance (MDR), worsen clinical treatment and contribute to the spread of the disease.

In the field of antimycobacterial inhibitors, there are several new classes of drugs proposed, *i.e.* chalcones [2] or α-pyrones [3], as well as new selective antimycobacterial targets like decaprenyl-phosphoryl-β-D-ribose2' epimerase (DprE1) [4] and Dihydrofolate Reductase (DHFR) [5].

It is also known that several imidazole derivatives show both antimycobacterial and antifungal activities [6-12] due to

*Address correspondence to this author at the Department of Chemistry and Pharmaceutical Sciences, P.le Europa 1, University of Trieste, 34127 Trieste, Italy; Tel: +39040-5587858; Fax: +3904052572; E-mail: dzampieri@units.it

1

the common target. In effect, the inhibition of cytochrome P450-dependent lanosterol 14α-demethylase (P450, CYP51) is the target of the azole antifungal agents but it was established, using genome DNA from *M. tuberculosis* (Mtb) H₃₇Rv strain, that a CYP51-like gene encodes a mycobacterial sterol 14α-demethylase (Mtb 14DM) which acts on 14α-methyl sterols and binds antifungal azole inhibitors of 14DM [13].

In our previous work [12], we already synthesized some 1-(2-aryl-2-phenylhydrazono)ethyl-1*H*-imidazole and 1-(2-aryl-2-phenylhydrazono)ethyl-1*H*-1,2,4-triazole derivatives gifted with moderate antifungal activity toward two *Candida spp.* (MIC range 8-64 µg/ml) and rather low antimycobacterial activity against Mtb H₃₇Rv strain (MIC range 16-128 µg/ml).

In order to explore the chemical space around the azole nucleus and the relevance of the aromatic elements for the antimycobacterial activity, we chose to retain the original structure of our previous derivatives and to replace the phenylhydrazine group with the corresponding, more lipophilic, 2,6-dichlorophenylhydrazine moiety, the dichlorophenyl ring is a key element not only in many well-known antifungal drugs such as miconazole, ketoconazole and zinoconazole [14], but also in some compounds gifted with antimycobacterial activity [15, 16], as depicted in Fig. (**1**).

By these assumptions we synthesized some new 1-(1-(aryl)-2-(2,6-dichlorophenyl)hydrazono)ethyl-1*H*-imidazole and 1*H*-1,2,4-triazole derivatives **2a-l** (Fig. **2**).

2. EXPERIMENTAL

2.1. Chemistry, General Remarks

Commercially available chemicals were of reagents grade and used as such. Melting points were determined with a Stuart SMP30 capillary apparatus, and are uncorrected. Reaction courses and product mixtures were routinely monitored by Thin-layer Chromatography (TLC) on silica gel precoated F₂₅₄ Merck plates. Infrared spectra in nujol mulls were recorded on a Jasko FT 200 spectrophotometer. Proton

nuclear magnetic resonance spectra (¹H-NMR) and carbon nuclear magnetic resonance spectra (¹³C-NMR) were obtained on a Varian Gemini 200 MHz spectrometer, a Jeol 270 MHz or a Varian 400 MHz; chemical shifts are reported in part per million (δ, ppm) in CDCl₃ solution (0.05% v/v TMS) or DMSO-d₆; D₂O has been added (1 drop) to assign NH protons. Coupling constants (J) are reported in Hz and the splitting abbreviations used are: s, singlet; d, doublet; dd, double doublet; t, triplet; dt, double triplet; q, quartet; m, multiplet; br, broad. ESI-MS spectra were obtained on a PE-API I spectrometer by infusion of a solution of the sample in ultrapure MeOH. NMR spectra are provided as Supplementary material. Chemdraw® software v. 12.0.3. was used for the chemical graphics and Marvinsketch® v. 17.1.2 (chemaxon mode) was used for estimated solubility data.
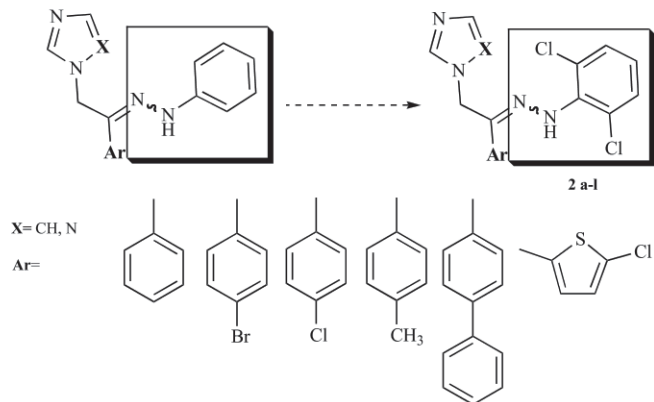
Fig. (2). The rationale for the synthesis of new 2,6-dichlorophenylhydrazine derivatives **2a-l**.

2.2. General Procedure for the Preparation of 2-(1H-Imidazol-1-yl)-1-(Aryl)Ethanone 1a-f

2.2.1. Synthesis of 2-(1H-Imidazol-1-yl)-1-(Phenyl) Ethanone 1a

In a 250 ml round bottom flask, 5.0 g of 2-bromo-1-phenylethanone (25 mmol) and 5.1 g (75 mmol) of imidazole in 100 ml of THF were left to react overnight at room tem-
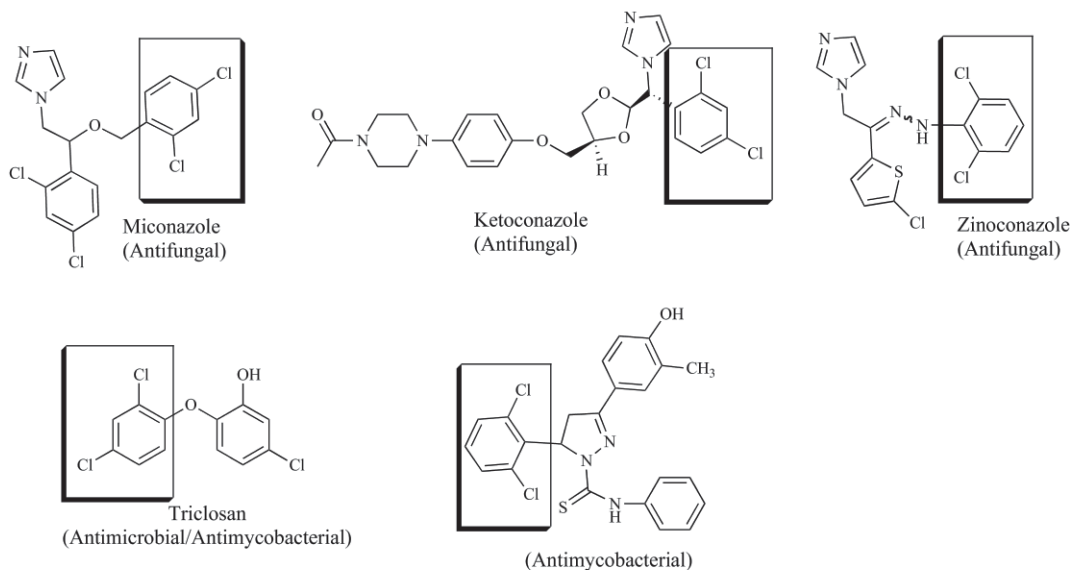
Fig. (1). Structures of some known antifungal and antimycobacterial compounds.

2

perature. The solvent was removed by rotary evaporation and the solid residue was taken up with CH_2Cl_2 and washed 3 times with distilled H_2O. The organic phases were collected, dried over anhydrous Na_2SO_4, filtered and evaporated under vacuum. The residue was crystallized from absolute EtOH.

Yield: 2.3 g, 48%; m.p. 114-116°C (lit. [17]: 116-118 °C); I.R. (nujol) ν_{max} 1688 (C=O) cm^{-1}; ^{1}H-NMR (CDCl$_3$, 200 MHz) δ(ppm): 5,34 (s, 2H, CH$_2$), 6.86 (s, 1H, imid.), 7.02 (s, 1H, imd.), 7.40-7.54 (m, 3H, arom. and 1H imid.), 7.87-7.80 (m, 2H, arom.).

2.2.2. Synthesis of 2-(1H-Imidazol-1-yl)-1-(4-Bromo-phenyl)Ethanone 1b

Yield: 67%; m.p. 162-165°C (lit. [18]: 163-164°C); I.R. (nujol) ν_{max} 1693 (C=O) cm^{-1}; ^{1}H-NMR (CDCl$_3$, 200 MHz) δ(ppm): 5.34 (s, 2H, CH$_2$), 6.89 (s, 1H, imid.), 7.09 (s, 1H, imid.), 7.61-7.66 (m, 3H, 2H arom. and 1H imid.), 7.78-7.82 (m, 2H, arom.).

2.2.3. Synthesis of 2-(1H-Imidazol-1-yl)-1-(4-Chloro-phenyl)Ethanone 1c

Yield: 77%; m.p. 150-156°C (lit. [17]: 152-156°C); I.R. (nujol) ν_{max} 1689 (C=O) cm^{-1}; ^{1}H-NMR (CDCl$_3$, 200 MHz) δ(ppm): 5.35 (s, 2H, CH$_2$), 6.90 (s, 1H, imid.), 7.08 (s, 1H, imid.), 7.45-7.51 (m, 3H, 1H imid. e 2H arom.), 7.86-7.91 (m, 2H, arom.).

2.2.4. Synthesis of 2-(1H-Imidazol-1-yl)-1-(4-Tolyl) Etha-none 1d

Yield: 79%; m.p. 118-123°C (lit. [17]: 133-137°C); I.R. (nujol) ν_{max} 1694 (C=O) cm^{-1}; ^{1}H-NMR (CDCl$_3$, 200 MHz) δ(ppm): 2.41 (s, 3H, CH$_3$), 5.35 (s, 2H, CH$_2$), 6.91-7.82 (m, 5H, 2H arom. and 3H imid.), 7.86 (d, 2H, arom.).

2.2.5. Synthesis of 1-([1,1'-Biphenyl]-4-yl)-2-(1H-Imidazol-1-yl)Ethanone 1e

Yield: 50%; m.p. 162-168°C (lit. [19]: 164-166°C); I.R. (nujol) ν_{max} 1694 (C=O) cm^{-1}; ^{1}H-NMR (CDCl$_3$, 200 MHz) δ(ppm): 5.45 (s, 2H, CH$_2$), 6.97 (s, 1H, imid.), 7.15 (s, 1H, imid.), 7.40-8.06 (m, 10H, 9H arom. and 1H imid.).

2.2.6. Synthesis of 1-(5-Chlorothiophen-2-yl)-2-(1H-Imidazol-1-yl)Ethanone 1f

Yield: 96%; m.p. 162-168°C; I.R. (nujol) ν_{max} 1672 (C=O) cm^{-1}; ^{1}H-NMR (DMSO-d6, 200 MHz) δ(ppm): 5.90 (s, 2H, CH$_2$), 7.43 (d, 1H, imid.), 7.69 (d, 2H, tiof.), 8.08 (d, 1H, imid.), 8.12 (s, 1H, imid.). ^{1}C-NMR (DMSO-d6, 200 MHz) δ(ppm): 52.9, 119.2, 127.6, 129.6, 133.0, 138.2, 139.4, 145.1, 194.3. MS (ESI$^+$): m/z 227 [MH$^+$] 229 [MH$^+$+2].

2.3. General Procedure for the Preparation of 2-(1H-1,2,4-Triazol-1-yl)-1-(aryl)Ethanone 1g-l

2.3.1. Synthesis of 2-Phenyl-1-(1H-1,2,4-Triazol-1-yl)Etha-none 1g

To a solution of 1.20 g (17.5 mmol) of 1,2,4-triazole in 30 ml of THF, and equimolar amount of NaH was added and the solution was left to stir for 30 minutes at room temperature; then 3.50 g (17.5 mmol) of 2-bromoacetophenone were added and the mixture was stirred until the reaction was completed. The solvent was removed by rotary evaporation and the residue was poured into distilled water, extracted with CH_2Cl_2 (3x100 ml). The organic phase was dried (Na$_2$SO$_4$), filtered and evaporated in vacuo to give a solid which was crystallized from absolute EtOH.

Yield: 25%; m.p. 110-115°C (lit. [20]: 117-118.5°C); I.R.(nujol) ν_{max} 1694 (C=O) cm^{-1}; ^{1}H-NMR (CDCl$_3$, 200 MHz) δ(ppm): 5.63 (s, 2H, CH$_2$), 7.42-7.89 (m, 5H, arom.), 7.91 (s, 1H, triaz.), 8.18 (s, 1H, triaz.).

2.3.2. Synthesis of 2-(4-Bromophenyl)-1-(1H-1,2,4-Triazol-1-yl)Ethanone 1h

Yield: 45%; m.p. 175-177°C (lit. [21]: 179-180°C); I.R. (nujol) ν_{max} 1688 (C=O) cm^{-1}; ^{1}H-NMR (CDCl$_3$, 200 MHz) δ(ppm): 5.62 (s, 2H, CH$_2$), 7.64-7.68 (m, 2H, arom.), 7.80-7.85 (m, 2H, arom.), 7.98 (s, 1H, triaz.), 8.22 (s, 1H, triaz.).

2.3.3. Synthesis of 2-(4-Chlorophenyl)-1-(1H-1,2,4-Triazol-1-yl)Ethanone 1i

A slight modification of the above procedure was adopted.

To a solution of 4.2 g (60.9 mmol) of 1,2,4-triazole in 30 ml of DMF in an ice-bath at 0°C, 2-bromo-1-(4-chlorophenyl)-ethanone (12.2 mmol) dissolved in a minimum amount of the same solvent was added in a dropwise manner. After the reaction was completed, the solvent was removed under vacuum and the residue was poured into ice-water and extracted with CH_2Cl_2 (3x) dried and filtered. The solution was evaporated to afford a residue which was crystallized from toluene.

Yield: 34%; m.p. 144-150°C (lit. [21]: 152-153°C); I.R. (nujol) ν_{max} 1691 (C=O) cm^{-1}; ^{1}H-NMR (CDCl$_3$, 200 MHz) δ(ppm): 5.96 (s, 2H, CH$_2$), 7.61-7.65 (m, 2H, arom.), 8.00-8.05 (m, 3H, 2H arom., e 1H triaz.), 8.48 (s, 1H, triaz.).

2.3.4. Synthesis of 2-(4-Tolyl)-1-(1H-1,2,4-Triazol-1-yl) Ethanone 1j

The same procedure of 1g was adopted.

Yield: 54%; m.p. 82-85°C (lit. [22]: 61-63°C); I.R. (nujol) ν_{max} 1678 (C=O) cm^{-1}; ^{1}H-NMR (CDCl$_3$, 200 MHz) δ(ppm): 2.41 (s, 3H, CH$_3$), 5.82 (s, 2H, CH$_2$), 7.28 (m, 2H, arom.), 7.83-7.87 (s, 2H, arom.), 7.96 (s, 1H, triaz.), 8.21 (s, 1H, triaz.).

2.3.5. Synthesis of 1-([1,1'-Biphenyl]-4-yl)-2-Bromo-ethanone 1k

The same procedure of 1i was adopted.

Yield: 30%; m.p. 159-162°C (lit. [21]: 172-173°C); I.R. (nujol) ν_{max} 1687 (C=O) cm^{-1}; ^{1}H-NMR (CDCl$_3$, 200 MHz) δ(ppm): 5.69 (s, 2H, CH$_2$), 7.24-7.74 (m, 7H, arom.), 8.00 (m, 2H, arom,), 8.04 (s, 1H, triaz.), 8.26 (s, 1H, triaz.).

2.3.6. Synthesis of 1-(5-Chlorothiophen-2-yl)-2-(1H-1,2,4-triazol-1-yl)Ethanone 1l

This compound was obtained following the same procedure of 1g, but using NaOH (half equivalent) instead of NaH as base.

Yield: 66%; m.p. 127-129°C; I.R. (nujol) ν_{max} 1682 (C=O) cm^{-1}; ^{1}H-NMR (CDCl$_3$, 200 MHz) δ(ppm): 7.07 (d,

1H, tioph. H-4, J= 3.66 Hz), 7.64 (d, 1H, tioph. H-3, J= 3.66 Hz), 8.03 (s, 1H, H-5 triaz.) 8.28 (s, 1H, H-3 triaz.). ^{13}C-NMR (DMSO-d6, 200 MHz) δ(ppm): 51.1, 119.4, 127.4, 130.6, 139.1, 142.1, 143.4, 151.3, 192.3. MS (ESI$^+$): m/z 228 [MH$^+$] 230 [MH$^+$+2].

2.4. General Procedure for the Synthesis of Derivatives 2a-l

A solution of 1-phenyl-2-(1H-imidazol-1-yl)-ethanone (1.0 g, 5.4 mmol) in 50 ml of ethanol, was treated with two drops of acetic acid. To the stirred solution, 2,6-dichlorophenylhydrazine hydrochloride (1.1 g, 6.4 mmol) in 50 ml of absolute ethanol was added dropwise and the reaction mixture was heated at reflux (CaCl$_2$ trap) for 6 h. Thereafter, the solvent was removed under reduced pressure and the residue was taken up with CH$_2$Cl$_2$ and washed with distilled water (3x50 ml). The collected organic phases were dried over anhydrous Na$_2$SO$_4$, filtered and evaporated under reduced pressure. The residue was crystallized from absolute ethanol.

2.4.1. Synthesis of (Z) 1-(2-(2-(2,6-Dichloro-phenyl)Hydrazono)-2-Phenylethyl)-1H-Imidazole, Chloride Salt 2a

This compound was obtained as hydrochloride directly after the reaction was completed, by crystallization from EtOH.

Ochre solid, yield: 45%; m.p. 107-109°C; I.R. (nujol) $_{vmax}$ 3403, 2720, 2667 cm^{-1}; ^{1}H-NMR (DMSO-d6, 270 MHz) δ(ppm): 6.11 (s, 2H, CH$_2$ Z-isomer 90% and 5.85 CH$_2$ E-isomer 10%), 7.24-8.10 (m, 11H, 3H imid., 8H arom.), 9.16 (s, 1H, NH D$_2$O exchanged), 10.80 (broad peak, NH$^+$ D$_2$O exchanged); MS (ESI$^+$): m/z 383 [MH$^+$] 385 [MH$^+$+2] [23].

2.4.2. Synthesis of (Z) 1-(2-(4-Bromophenyl)-2-(2-(2,6-Dichlorophenyl)Hydrazono)-ethyl)-1H-Imidazole, 2b

Yellow solid, yield: 32%; m.p. 220-220°C; I.R. (nujol) $_{vmax}$ 3450 cm^{-1}; ^{1}H-NMR (DMSO-d6, 200 MHz) δ(ppm): 5.80 (s, 2H, CH$_2$), 7.19-7.81 (m, 9H, 2H imid., 7H arom.), 9.27 (s, 1H, H$_2$ imid.), 9.77 (s, 1H, NH D$_2$O exchanged); MS (ESI$^+$): m/z 425 [MH$^+$], 427 [MH$^+$+2] [23].

2.4.3. Synthesis of (Z) 1-(2-(4-Chorophenyl)-2-(2-(2,6-Dichlorophenyl)Hydrazono)-ethyl)-1H-Imidazole, 2c

Light-yellow solid, yield: 59%; m.p. 216-218°C; I.R. (nujol) $_{vmax}$ 3430 cm^{-1}; ^{1}H-NMR (DMSO-d6, 200 MHz) δ(ppm): 5.80 (s, 2H, CH$_2$), 7.20-7.86 (m, 9H, 2H imid., 7H arom.), 9.25 (s, 1H, H$_2$ imid.), 9.72 (s, 1H, NH, D$_2$O exchanged); MS (ESI$^+$): m/z 381 [MH$^+$], 383 [MH$^+$+2] [23].

2.4.4. Synthesis of (E) 1-(2-(2-(2,6-Dichloro-phenyl)Hydrazono)-2-(p-Tolyl)Ethyl)-1H-Imidazole, 2d

Ochre solid, yield: 50%; m.p. 158-160°C; I.R. (nujol) $_{vmax}$ 3436 cm^{-1}; ^{1}H-NMR (CDCl$_3$, 400 MHz) δ(ppm): ^{1}H-NMR (CDCl$_3$-TMS) δ(ppm): 2.37 (s, 3H, CH$_3$), 4.95 (s, 2H, CH$_2$ E-isomer 90% and 5.26 ppm CH$_2$ Z-isomer 10%), 6.91 (t, 1H, arom., J= 8.0 Hz), 6.99 (s, 1H, H$_4$ imidaz.), 7.08 (m, 2H, arom.), 7.26 (m, 4H, arom.), 7.55 (s, 1H, H$_5$ imid.), 7.61 (s, 1H, H$_2$ imid.), 8.94 (s, 1H, NH D$_2$O exchanged); MS (ESI$^+$): m/z 360 [MH$^+$], 362 [MH$^+$+2] [23].

2.4.5. Synthesis of (Z)-1-(2-([1,1'-Biphenyl]-4-yl)-2-(2-(2,6-Dichlorophenyl)Hydrazono)ethyl)-1H-Imidazole, Chloride Salt 2e

This compound was obtained as hydrochloride directly after the reaction was completed, by spontaneous crystallization from abs. EtOH.

Ochre solid, yield: 55%; m.p. 159-161°C; I.R. (nujol) $_{vmax}$ 3415, 2710, 2664 cm^{-1}; ^{1}H-NMR (DMSO-d6, 270 MHz) δ(ppm): 6.14 (s, 2H, CH$_2$ Z-isomer 90% and 5.88 ppm CH$_2$ E-isomer 10%), 7.28 (t, 2H, arom.), 7.50-7.85 (m, 8H, arom. + imidaz.), 7.96 (d, 2H, arom, J= 8Hz), 8.16 (d, 2H, arom, J= 8Hz), 9.17 (s, 1H, H$_2$ imidaz.), 9.60 (s, 1H, NH D$_2$O exchanged), 10.70 (broad peak, NH$^+$ D$_2$O exchanged); MS (ESI$^+$): m/z 459 [MH$^+$], 461 [MH$^+$+2].

2.4.6. Synthesis of (E)-1-(2-(5-Chlorothiophen-2-yl)-2-(2-(2,6-Dichlorophenyl)Hydrazono)ethyl)-1H-Imidazole, Chloride Salt 2f

This compound was obtained as hydrochloride directly after the reaction was completed, by spontaneous crystallization from abs. EtOH.

Light-yellow solid, yield: 65%; m.p. 200-208°C dec.; I.R. (nujol) $_{vmax}$ 3447, 2723, 2672 cm^{-1}; ^{1}H-NMR (DMSO-d6, 400 MHz) δ(ppm): 5.80 (s, 2H, CH$_2$), 7.06 (d, 1H, tioph.-H$_4$, J= 4.0 Hz), 7.22 (t, 1H, arom. phenylhydr. J= 8.0 Hz), 7.43 (d, 1H, tioph.-H$_3$, J= 4.0 Hz), 7.49 (d, 2H, arom. phenyl-hydr., J= 8.0 Hz), 7.61 (s, 1H, H$_4$ imidaz.) 7.68 (s, 1H, H$_5$ imidaz.), 9.34 (s, 1H, H$_2$ imidaz.), 9.87 (s, 1H, NH, D$_2$O exchanged); 14.9 (broad peak, NH$^+$, D$_2$O exchanged); ^{13}C-NMR (DMSO-d6, 400 MHz): 42.2, 109.9, 120.8, 122.2, 125.3, 127.7, 127.9, 129.3, 129.6, 130.8, 134.4, 136.2, 138.3, 141.6, 157.4; MS (ESI$^+$): m/z 423 [MH$^+$], 425 [MH$^+$+2]. [14]

2.4.7. Synthesis of (Z/E)- 1-(2-(2-(2,6-Dichloro-phenyl)Hydrazono)-2-Phenylethyl)-1H-1,2,4-Triazole 2g

Orange solid, yield: 25%; m.p. 110-112°C; I.R. (nujol) $_{vmax}$ 3420 cm^{-1}; ^{1}H-NMR (CHCl$_3$, 200 MHz) δ(ppm): 5.26 (s, 2H, CH$_2$ isomer E-minor-), 5.50 (s, 2H, CH$_2$ isomer Z-major-), 6.90-8.30 (m, 10H, 2H triaz., 8H arom.), 9.35 (s, 1H, NH D$_2$O exchanged); MS (ESI$^+$): m/z 347[MH$^+$], 349 [MH$^+$+2].

2.4.8. Synthesis of (Z) 1-(2-(4-Bromophenyl)-2-(2-(2,6-Dichlorophenyl)Hydrazono)-Ethyl)-1H-1,2,4-Triazole 2h

Light-orange solid, yield: 55%; m.p. 88-90°C; I.R. (nujol) $_{vmax}$ 3435 cm^{-1}; ^{1}H-NMR (CDCl$_3$, 400 MHz) δ(ppm): 5.45 (s, 2H, CH$_2$), 6.97 (t, 1H, arom., J= 8.0 Hz), 7.33 (d, 2H, arom., J= 8Hz), 7.52 (d, 2H, arom., J= 8 Hz), 7.66 (d, 2H, arom., J= 8 Hz), 8.05 (s, 1H, H$_5$ triaz.), 8.27 (s, 1H, H$_2$ triaz.), 9.31 (s, 1H, NH D$_2$O exchanged); MS (ESI$^+$): m/z 426[MH$^+$], 428 [MH$^+$+2].

2.4.9. Synthesis of (Z) 1-(2-(4-Chorophenyl)-2-(2-(2,6-Dichlorophenyl)hydrazono)-Ethyl)-1H-1,2,4-Triazole 2i

Light-brown solid, yield: 33%; m.p. 105-107°C; I.R. (nujol) $_{vmax}$ 3400 cm^{-1}; ^{1}H-NMR (CHCl$_3$, 200 MHz) δ(ppm): 5.67 (s, 2H, CH$_2$), 6.92 (t, 1H, arom. phenylhydr. J= 8.0 Hz), 7.27 (d, 2H, arom. phenylhydr., J= 8.0 Hz), 7.54 (d, 2H, arom. p-subs., J= 8.0 Hz), 7.95 (d, 2H, arom. p-subs., J= 8.0 Hz), 8.03 (s, 1H, H$_5$ triaz.) 8.27 (s, 1H, H$_3$ triaz.), 9.37 (s,

1H, NH D$_2$O exchanged); MS (ESI$^+$): m/z 382[MH$^+$], 384 [MH$^+$+2].

2.4.10. Synthesis of (Z)-1-(2-(2-(2,6-Dichlorophenyl) Hydrazono)-2-(p-Tolyl)Ethyl)-1H-1,2,4-Triazole 2j

Dark-orange solid, yield:45%; m.p. 74-78°C; I.R. (nujol) νmax 3432 cm^{-1}; ^{1}H-NMR (CDCl$_3$, 200 MHz) δ(ppm): 2.47 (s, 3H, CH$_3$), 5.68 (s, 2H, CH$_2$), 6.92 (t, 1H, arom. phenylhyidr. J= 8.0 Hz), 7.29 (d, 2H, arom. phenylhyidr. J= 8.0 Hz), 7.35 (d, 2H, arom. p-subs., J= 8.0 Hz), 7.95 (d, 2H, arom. p-subs., J= 8.0 Hz), 8.03 (s, 1H, H$_5$ triaz.) 8.27 (s, 1H, H$_3$ triaz.), 9.25 (s, 1H, NH D$_2$O exchanged); MS (ESI$^+$): m/z 361 [MH$^+$], 363 [MH$^+$+2].

2.4.11. Synthesis of (Z)-1-(2-([1,1'-Biphenyl]-4-yl)-2-(2-(2,6-Dichlorophenyl)Hydrazono)Ethyl)-1H-1,2,4-Triazole 2k

Yellow solid, yield: 40%; m.p. 170-172°C; I.R. (nujol) νmax 3430 cm^{-1}; ^{1}H-NMR (CDCl$_3$, 200 MHz) δ(ppm): 5.53 (s, 2H, CH$_2$), 6.90-7.95 (m, 12H, arom.), 8.09 (s, 1H, H$_5$ triaz.) 8.33 (s, 1H, H$_3$ imid.), 9.38 (s, 1H, NH D$_2$O exchanged); MS (ESI$^+$): m/z 423 [MH$^+$], 425 [MH$^+$+2].

2.4.12. Synthesis of (Z)-1-(2-(5-Chlorothiophen-2-yl)-2-(2-(2,6-Dichlorophenyl)Hydrazono)Ethyl)-1H-1,2,4-Triazole 2l

Yellow solid, yield: 34%; m.p. 175-177°C; I.R. (nujol) νmax 3434 cm^{-1}; ^{1}H-NMR (CDCl$_3$, 200 MHz) δ(ppm): 5.40 (s, 2H, CH$_2$), 6.87 (d, 1H, tioph.-H$_4$, J= 4.0 Hz), 6.96 (t, 1H, arom. phenylhydr. J= 8.0 Hz), 7.04 (d, 1H, tioph.-H$_3$, J= 4.0 Hz), 7.34 (d, 2H, arom. phenylhydr., J= 8.0 Hz), 8.06 (s, 1H, H$_5$ triaz.) 8.24 (s, 1H, H$_3$ triaz.), 9.47 (s, 1H, NH, D$_2$O exchanged); MS (ESI$^+$): m/z 388 [MH$^+$], 390 [MH$^+$+2].

2.5. Biological Evaluation

2.5.1. Antimycobacterial Studies

Mycobacterium tuberculosis H$_{37}$Ra ATCC 25197 were maintained on slants of Lowenstein-Jensen Medium (Difco, Becton Dickinson, Sparks, MD, USA), at 37°C in an atmosphere of 5% CO$_2$. An aliquot of these cultures transferred in Middlebrook 7H9 broth (Difco), supplemented with 10% ADC (albumin, dextrose, catalase, Difco) and 0.04% Tween 80 to avoid clump formation and incubated at 37°C in 5% CO$_2$. Cells were harvested by centrifugation, resuspended in saline until a 1 McFarland density (1x10^8 cells/ml) was reached, diluted 1:20 in Middlebrook 7H9 broth with 10% ADC and 0.04% Tween 80, and sonicated in a bath-type sonicator to disrupt the clumps. The absence of clumps was also verified by a Zhiel-Neelsen staining. In order to confirm the title of inoculum employed, the bacterial suspensions were appropriately diluted and seeded on plates of Middlebrook 7H11 agar supplemented with 10% OADC (oleic acid, albumin, dextrose, catalase, Difco). The plates were incubated at 37°C for 28 days and then was determined on the number of colonies developed.

2.5.1.1. Staging of the Solutions of the Test Compounds

The test compounds were dissolved in DMSO at a concentration of 1-5 mg/ml, depending on their solubility and stored at -20°C until use. Compounds were subsequently diluted in Middlebrook 7H9 broth with ADC 10% to obtain a final concentration of 128 µg/ml and further diluted 1:2 in the same medium until the concentration of 0.25 µg/ml.

2.5.1.2. Determination of Antimycobacterial Activity

MIC of the tested compounds were determined against *Mycobacterium tuberculosis* H$_{37}$Ra ATC 25197 by the resazurin microtiter assay as previously described [24, 25] with slights modifications. 50 µL of each solution of the tested compounds prepared as described above, were transferred into individual wells of 96-well plates and then 50 µL of the suspensions of mycobacteria previously arranged were added, in order to obtain a range of concentrations of the test compounds between 0.125 and 64 µg/ml. Each concentration was assayed in quadruplicate. The plates were incubated at 37°C in 5% CO$_2$ for 7 days. 30 µL of resazurin (Sigma Aldrich Co., St. Louis, MO) solution prepared at 0.01% (wt/vol) in distilled water, filter sterilized and stored at 4°C, was added to each well, incubated 24-48 h at 37°C, and assessed for color development. The change of color from blue to pink indicates bacterial growth. Therefore, the minimum inhibitory concentration (MIC) was attributed to the lower concentration of the test compound to inhibit the color change of resazurin. Isoniazid (INH, Sigma Aldrich) was used as reference compound. Each determination was repeated twice under the conditions described.

2.5.2. Cytotoxicity Studies

Vero cells line used in this study were obtained from the Biobanking of the Veterinary Resources (BVR, IZLER, Brescia, Italy). Cells were grown and maintained in RMPI 1640 medium (Gibco, Thermo Fisher Scientific, Waltham, MA) supplemented with 2mM l-glutamine (Gibco), penicillin 100 IU/ml (Gibco), streptomycin 100 µg/ml (Gibco), and 10% fetal bovine serum (Gibco). Cultures were maintained at 37°C in 5% CO$_2$. For cytotoxicity experiments, cells were seeded in 96-well plastic microtiter plates (Falcon, Becton Dickinson) containing no antibiotics and the testing compound, or INH as reference compound, at concentrations ranging between 0.2 and 1000 µg/ml, depending on their solubility in DMSO, and incubated at 37°C in 5% CO$_2$. Cells were observed for morphological changes at 24, 48 and 72 h of incubation. After 72 h the effects on the proliferation of Vero cells were determined by the tetrazolium based colorimetric 3-(4,5-dimethyl-2-thiazolyl)-2,5-diphenyl-2H-tetrazolium bromide (MTT, Sigma Aldrich) assay. The 50% cell-inhibitory concentration (CC$_{50}$) reduced by 50% the optical density values (OD$_{540,690}$) with respect to control no-treated cells, and was obtained using an automatic plate reader.

2.6. Molecular Modeling

The optimized structure of **2e** and **2f** was docked into the binding pockets of the 14DM by applying a consolidated procedure [26] accordingly, it will be described here only briefly. All docking experiments were performed with Autodock 4.3/Autodock Tools 1.4.6 [27] on a win64 platform. DS was employed to define the size of the binding site, using an opening site of 10 Å and a grid size of 0.7 Å. The dimensions of the Autodock grid box, based on the cavity identified by DS, was large enough to cover all possible rotations of each ligand. Van der Waals interactions were

modelled with the Amber 12-6 and 12-10 Lennard-Jones parameters, respectively, while the distance-dependent relative permittivity of Mehler and Solmajer [28] was applied in the generation of the electrostatic grid maps. A total of 300 Monte Carlo/simulated annealing (MC/SA) runs were performed, with 100 constant-temperature cycles for simulated annealing. The GB/SA implicit water model [29] was used in these calculations to mimic the solvated environment. The angles of the side chains and the rotation of the angles φ and ψ were set free during the calculations, while all others parameters of the MC/SA algorithm were kept as default. The structures of the two compounds were subjected to cluster analysis with a 1 Å tolerance for an all-atom root-mean-square (rms) deviation from a lower energy structure representing each cluster family. The resulting docked conformations were clustered and visualized; then, for each compound, only the molecular conformation satisfying the combined criteria of having the lowest (i.e., more favorable) Autodock energy and belonging to a highly populated cluster was selected to carry for further modeling.

The ligand/protein complex obtained from the docking procedure was further refined in Amber 14 [30] using the Quenched Molecular Dynamics (QMD) method. According to QMD, 1 ns MD simulations at 300 K were employed to sample the conformational space of each ligand/protein complex in the GB/SA continuum solvation environment [25]. The integration step was equal to 1 fs. After each picosecond, each system was cooled to 0 K, and the structure was extensively minimized and stored. To prevent global conformational changes of the protein, the backbone atoms of the protein binding site were constrained by a harmonic force constant of 100 kcal/Å, whereas the amino acid side chains and the ligands were allowed to move without any constraint. The best energy configuration of each complex resulting from the previous step was subsequently solvated by a cubic box of TIP3P [31] water molecules extending at least 10 Å in each direction from the solute. The system was neutralized and the solution ionic strength was adjusted to the physiological value of 0.15 M by adding the required amounts of Na^+ and Cl^- ions. Each solvated system was relaxed by 500 steps of steepest descent followed by 500 other conjugate-gradient minimization steps and then gradually heated to a temperature of 300 K in intervals of 50 ps of NVT MD, using a Verlet integration time step of 1.0 fs. The Langevin thermostat was used to control temperature, with a collision frequency of 2.0 ps-1. The SHAKE method [32] was used to constrain all of the covalently bound hydrogen atoms, while long-range nonbonded van der Waals interactions were truncated by using dual cutoffs of 6 and 12 Å. The Particle Mesh Ewald (PME) method [33] was applied to treat long-range electrostatic interactions. The protein was restrained with a force constant of 2.0 kcal/ (mol Å), and all simulations were carried out with periodic boundary conditions.

The density of the system was subsequently equilibrated via MD runs in the isothermal − isobaric (NPT) ensemble, with isotropic position scaling and a pressure relaxation time of 1.0 ps, for 50 ps with a time step of 1 fs. All restraints on the protein atoms were then removed, and each system was further equilibrated using NPT MD runs at 300 K, with a pressure relaxation time of 2.0 ps. Three equilibration steps were performed, each 5 ns long and with a time step of 2.0 fs. To check the system stability, the fluctuations of the rmsd of the simulated position of the backbone atoms of the σ1 receptor with respect to those of the initial protein were monitored. All chemicophysical parameters and rmsd values showed very low fluctuations at the end of the equilibration process, indicating that the systems reached a true equilibrium condition. The equilibration phase was followed by a data production run consisting of 50 ns of MD simulations in the canonical (NVT) ensemble. Only the last 25 ns of each equilibrated MD trajectory were considered for statistical data collections. A total of 1250 trajectory snapshots were analyzed for each ligand/protein complex.

The binding free energy, ΔGbind, between the two compounds and the 14DM was estimated by resorting to the MM/PBSA approach implemented in Amber 14. According to this well-validated methodology, [12, 34-36] the free energy was calculated for each molecular species (complex, receptor, and ligand), and the binding free energy was computed as the difference:

$$\Delta Gbind = Gcomplex - (Greceptor + Gligand) = \Delta EMM + \Delta Gsol - T\Delta S \quad \textbf{(Eq. 1)}$$

The molecular mechanics energy ΔEMM was calculated as the sum of the van der Waals and electrostatic interactions:

$$\Delta EMM = \Delta EVDW + \Delta EELE \quad \textbf{(Eq. 2)}$$

The solvation free energy term ΔGsolv was composed of the polar and nonpolar contributions:

$$\Delta Gsolv = \Delta GPB + \Delta GNP \quad \textbf{(Eq. 3)}$$

The conformational entropy (translation, rotation, and vibration) upon ligand binding (−TΔS in Eq. 1) was estimated using normal-mode analysis [37] with the Nmode module of Amber 14. To minimize the effects due to different conformations adopted by individual snapshots, and due to the high computational demand of this approach, we averaged the estimation of entropy over MD 250 snapshots for each molecular complex that were evenly extracted from the last 25 ns of each corresponding MD trajectory.

The per residue binding free energy decomposition was performed exploiting the MD trajectory of each given compound/receptor complex, with the aim of identifying the key residues involved in the ligand-receptor interaction. This analysis was carried out using the MM/GBSA approach [29a], and was based on the same snapshots used in the binding free energy calculation.

All simulations were carried out using Pmemd modules of Amber 14, running on our own CPU/GPU calculation cluster.

3. RESULTS AND DISCUSSION

3.1. Chemistry

Some new 1-(1-(aryl)-2-(2,6-dichlorophenyl)hydrazono) ethyl-1H-imidazole and 1H-1,2,4-triazole derivatives **2a-l** including the zinoconazole, 1-(2-(5-chlorothiophen-2-yl)-2-(2-(2,6-dichlorophenyl)hydrazono)ethyl)-1H-imidazole **2f** and its triazole analogue 1-(2-(5-chlorothiophen-2-yl)-2-(2-
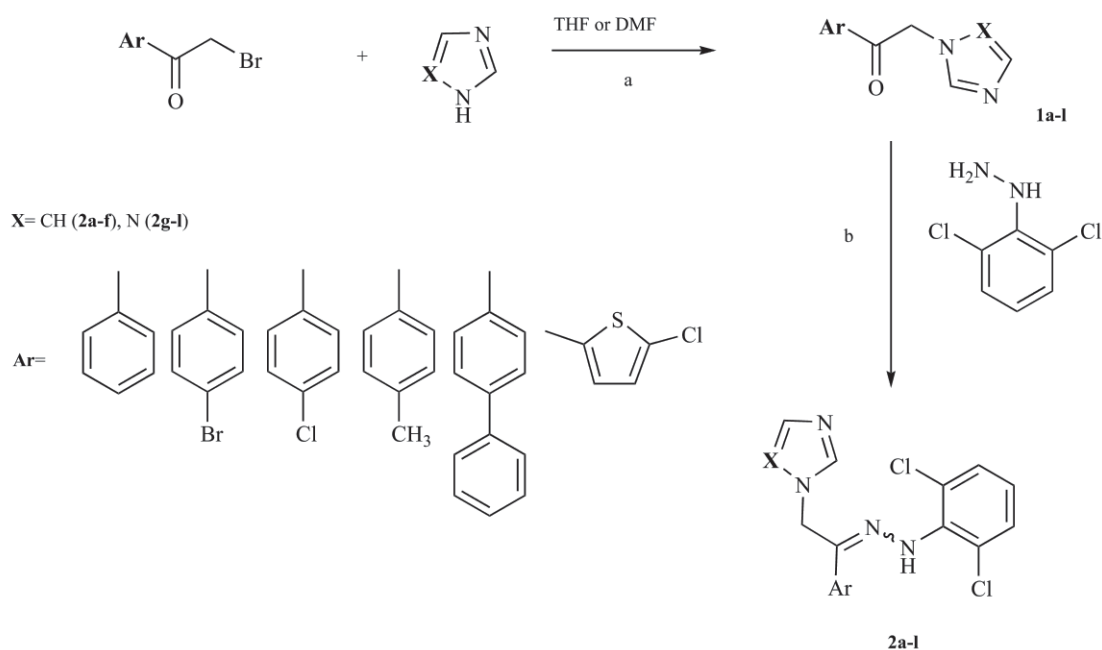
Scheme 1. Synthesis of the title compounds **2a-l**. Reagents and conditions: a) rt or 0°C, eventually NaH; b) EtOH$_{abs}$ (H$^+$cat), reflux.

(2,6-dichlorophenyl)hydrazono)ethyl)-1*H*-1,2,4-triazole **2l** were synthesized as depicted in Scheme **1**. The synthesis was carried out by treating the corresponding substituted 2-bromo-1-arylethanones, with an excess of imidazole or 1,2,4-triazole, in THF or DMF as solvent, to obtain the key intermediates 1-aryl-2-(1*H*-imidazol-1-yl)ethanones **1a-f** and 1-aryl-2-(1*H*-1,2,4-triazol-1-yl)ethanones **1g-l**, respectively. These intermediates were reacted with 2,6-dichlorophenyl hydrazine in refluxing ethanol (H$^+$ cat.) to obtain the final substituted 1-(1-(aryl)-2-(2,6-dichlorophenyl)hydrazono) ethyl-1*H*-imidazole and 1*H*-1,2,4-triazole derivatives **2a-l**.

All the title compounds were characterized by IR, NMR, mass spectral data (Table **1**, experimental session and supplementary material) and the results are consistent with the proposed structures.

The compounds exist as possible *Z* and *E* geometric isomers. From ^{1}H-NMR data and in accordance with the literature [14] we assigned the *Z/E* configuration to the final compounds. When the methylene protons appear as singlet, at lower fields, the configuration corresponds to the *Z* geometric isomer (E for **2f** and **2l**), indeed, in this configuration the CH$_2$ protons appear to be more deshielded by the closer presence of the hydrazine nitrogen atom. In some cases, the percentage of each isomer was calculated using the integral values of each singlet pair.

3.2. Biological Activity

3.2.1. Antimycobacterial Activity

In order to evaluate the effect of the replacement of the phenylhydrazine group of our previously synthesized compounds, with the corresponding 2,6-dichlorophenylhydrazine moiety on the antimycobacterial activity, we tested the derivatives **2a-l** towards a strain of Mtb H$_{37}$Rv and the MIC of the titled compounds are reported in Table **2**.

The data obtained for the imidazole sub-series **2a-f** revealed MIC values ranging from 4 to 32 μg/ml, with the best values of 4 μg/ml for compound **2f** (zinoconazole) and 8 μg/ml for the 4-methyl and 4-phenyl derivatives **2d** and **2e**. Regarding the triazole derivative **2g-l** the MIC range turned out to be 32 - >64 μg/ml, showing a moderate mycobacteria growth inhibition.
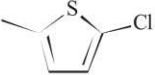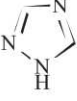
The results indicate that the triazole ring lead to a low antimycobacterial activity compared to the imidazole series, moreover, we can assert that the substitution of the phenyl-hydrazine group of our original structure, with the more lipophilic 2,6-dichlorophenylhydrazine, improve the antimycobacterial activity as well as the electron donating substituents, methyl and phenyl, in the 4- position of the phenyl ring (**2d** and **2e**).

We can speculate that both the imidazole and 2,6-dichlorophenylhydrazine moieties are gifted with more lipophilic character than the corresponding triazole and phenyl-hydrazine rings, with values greater than 1.0 point in terms of cLogP, cLogD and cLogS, compared to the original des-Cl compounds, as reported in Table **3**. This increased lipophilicity could be responsible for better interaction of imidazole sub-series (**2a-f**) with the waxy layer of the mycobacteria cell-wall and to penetrate more effectively into the cell to reach the target.
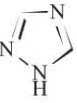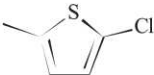
3.2.2. Cytotoxicity Study

In order to evaluate the safe cytotoxic profile of the target compounds **2a-l**, we performed a cytotoxicity assay towards mammalian Vero cells. We reported, in Table **2**, the Selectivity Index (S.I.) as an evaluation of the selectivity of our molecules between eukaryotic and mycobacterial cells, thus a value of safety of our titled compounds. According to a study of Hartkoorn and coworkers [38], on the drug susceptibility of TB, antimycobacterial activity is considered to be specific when the selectivity index is >10. In the current report, compound **2e** exhibited the highest selectivity index of 15, indicating its potential as an antitubercular agent, and thus it should be investigated further.

7

Table 1.   Characterization of title compounds 2a-l.

Entry	Het	Ar	Formula	M.p. (°C)[b]	Yield (%)[c]
2a	imidazole	Ph	$C_{17}H_{15}Cl_3N_4$[a]	107-109	45
2b		4-BrPh	$C_{17}H_{13}BrCl_2N_4$	220-222	32
2c		4-ClPh	$C_{17}H_{13}Cl_3N_4$	216-218	59
2d		4-CH₃Ph	$C_{18}H_{16}Cl_2N_4$	158-160	50
2e		4-PhPh	$C_{23}H_{19}Cl_3N_4$[a]	159-161	55
2f		5-methyl-2-chlorothiophene	$C_{21}H_{16}Cl_4N_4S$[a]	200-208	65
2g	triazole	Ph	$C_{17}H_{13}Cl_2N_5$	110-112	25
2h		4-BrPh	$C_{17}H_{12}BrCl_2N_5$	88-90	55
2i		4-ClPh	$C_{17}H_{12}Cl_3N_5$	105-107	33
2j		4-CH₃Ph	$C_{18}H_{15}Cl_2N_5$	74-78	45
2k		4-PhPh	$C_{23}H_{17}Cl_2N_5$	170-172	40
2l		5-methyl-2-chlorothiophene	$C_{21}H_{15}Cl_3N_4S$	175-177	34

[a]Obtained as hydrochlorides; [b]EtOH_abs; [c]Yields of the products in final step.

Table 2.   Antimycobacterial activity and cytotoxicity of title compounds 2a-l.

Entry	Het	Ar	MT H₃₇Rv (MIC)	VERO (CC₅₀)	S.I.[b]
			µg/ml		
2a	imidazole	Ph	32	58	1.8
2b		4-BrPh	16	18	1.1
2c		4-ClPh	16	19	1.2
2d		4-CH₃Ph	8	<15.6	1.9
2e		4-PhPh	8	115	15
2f		5-methyl-2-chlorothiophene	4	<15.6	3.9
2g	triazole	Ph	32	35	1.1
2h		4-BrPh	32	368	12
2i		4-ClPh	32	177	5.5
2j		4-CH₃Ph	>64	>500	>7.8
2k		4-PhPh	32	>500	15
2l		5-methyl-2-chlorothiophene	>64	>500	7.8
INH[a]	-	-	0.062	>7000	-

[a]Isoniazid as reference drug; [b]Selectivity Index (CC₅₀/MIC).

Table 3. cLogP, cLogD$_{7.4}$ and cLogS$_{7.4}$ of title compounds 2a-l, in comparison to des-Cl derivatives. (Marvinsketch® software v. 17.1.2 chemaxon mode).

Entry	cLogP	cLogD$_{7.4}$	cLogS$_{7.4}$
2a	4.18	4.71	-5.00
2b	4.98	5.47	-5.91
2c	4.70	5.18	-5.68
2d	4.65	5.15	-5.49
2e	5.87	6.38	-7.21
2f	4.45	5.16	-6.37
2g	3.69	4.22	-5.34
2h	4.49	4.98	-6.25
2i	4.21	4.69	-6.02
2j	4.16	4.66	-5.83
2k	5.38	5.89	-7.55
2l	3.96	4.71	-6.71
Des-Cl series	2.66 to 4.83[*]	2.66 to 4.76[*]	-3.58 to -6.21[*]

[*]Range value.

3.3. Molecular Docking Study

Given the presence of the azole ring, able to positively interact with a heme prosthetic group, we reasoned that the cytochrome P450 14α-sterol demethylase from *Mycobacterium tuberculosis* (Mtb 14DM) can be a plausible target for our compounds for exerting their antimycobacterial activity. Therefore, an extensive molecular modeling study has been carried out with the aim to support binding mode, the Mtb 14DM inhibition mechanism, and identification of the structural features of the active molecules from series of synthesized compounds. Accordingly, a well-validated Molecular Dynamics approach [19, 34-36] was performed for the more active compounds, **2e** and **2f**, with the aim to investigate the possible interactions with Mtb 14DM. The available crystallographic structure of the 14DM (pdb code 1EA1) in complex with Fluconazole [39], was used for these computational studies.

To check whether our docking procedure complied with the requirements of generating a correct docked conformation, we applied the same docking protocol to Fluconazole. This basically consisted in removing Fluconazole from the Mtb 14DM active site, ex novo building a molecular model for this compound, applying a conformational search procedure, and finally docking it back into the enzyme binding pocket. The best-docked structure was then compared with the binding pose of Fluconazole in the crystal structure. Fig. (**SI1**) (Supporting Information) gives a graphic view of the successful results of this comparison since the values of the root-mean-square deviation (RMSD) between docked and crystal structure is 0.26 Å. Based on these results, and on the fact that this approach was already successfully applied to different protein/ligand complexes, [26-44] we continued by applying the docking protocol for compounds **2e** and **2f**.

As a result of the applied docking procedure, we obtained a common binding mode for both compounds analysed in the 14DM active site (Fig. **3A-C**). The active site residues interacting with the inhibitors consisted of the β1-5-N-terminus of helix B' (residues 76-84), which constitutes the dome of the active site, meander 1 (residues 87-94), the C-terminus of helix F (residues 172-179), helix I (residues 249-261), β6–1 (residues 321-326), and β6–2 (residues 431-435). According to the procedure adopted, the imidazole ring is positioned almost perpendicular to the porphyrin plane, with a ring nitrogen atom coordinated to the haem iron. The analysis of the MD trajectories revealed that the average distance between N3 of the azole ring and the haem iron is 2.03 ± 0.05 Å for **2e** and 2.00 ± 0.03 Å for **2f**, respectively, in good agreement with that found in the crystal structure of 14DM complexed with other azole inhibitors [45].

Moreover, the 2,4-dichlorophenyl ring, common for both inhibitors, is perfectly nestled in a hydrophobic cavity of the binding pocket spanning residues A73, A75, Y76, F78, and L321 while the other aromatic moieties of the molecules, the biphenyl group of **2e** and the substituted thiophene ring of **2f**, are aptly encased in the other hydrophobic cavity of the 14DM binding site and the protein residues lining this subsite are I82, F83, L172, F255, A256 and V434 (Fig. **3B** and **3C**).

Deeper and more quantitative information about the forces involved in substrate binding can be obtained by analyzing the values of the free energy of binding, ΔG$_{bind}$ and its components (Fig. **3D**). For both compounds, the intermolecular van der Waals and the electrostatics (ΔE$_{vdW}$ + ΔE$_{ele}$) provided both important, favourable contribution to the binding (-55.71 kcal/mol for **2e** and –56.34 kcal/mol for **2f**), while the solvation free energy (ΔG$_{PB}$ + ΔG$_{NP}$) yielded an
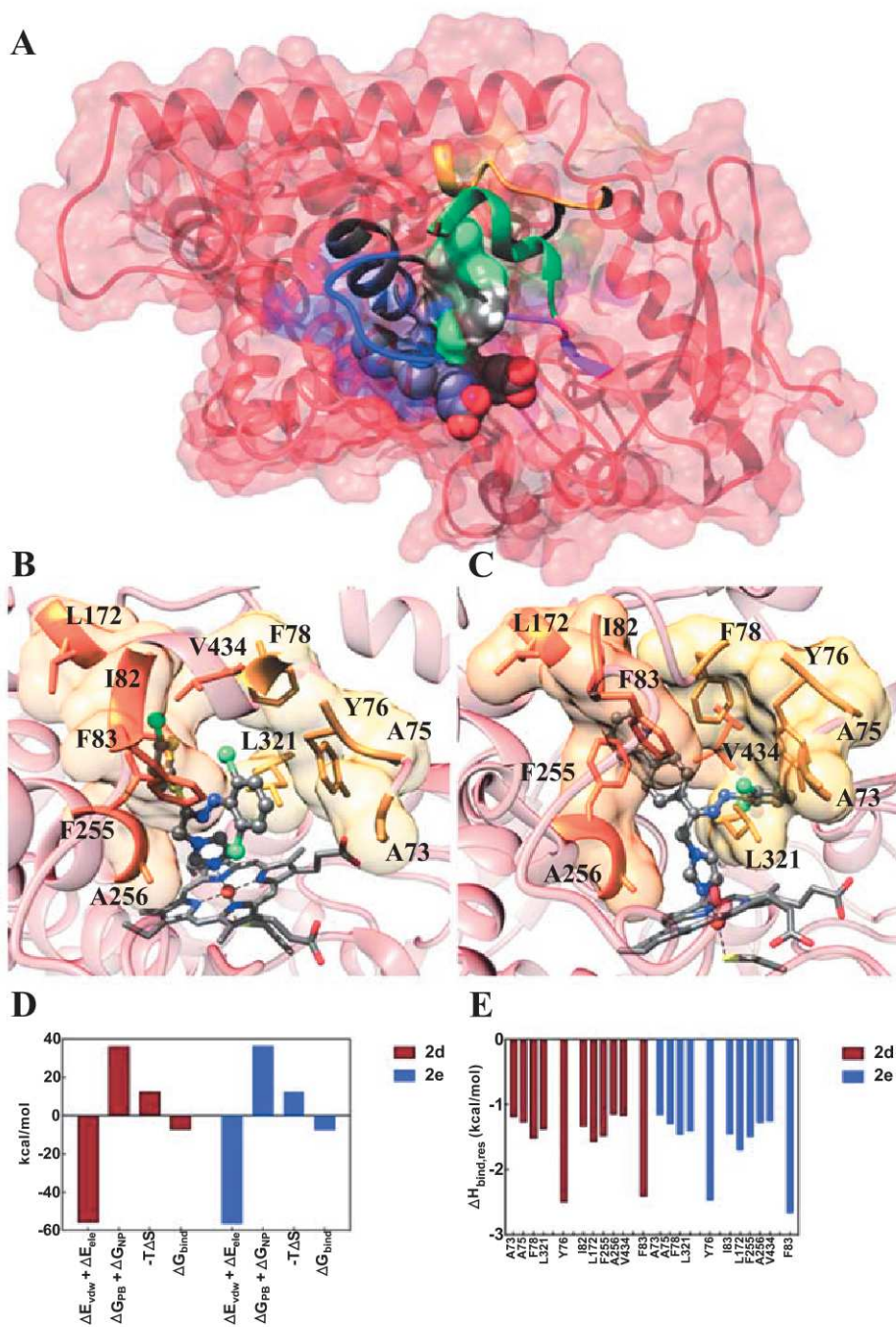
9

Fig. (3). A) Overall view of the MT 14DM/**2f** complex highlighting the structural motif of the MT 14DM: β1-5-B' (residues 76-84, green), meander 1 (87-94, blue), helix F (172-179, yellow), helix I (249-261, grey), β6–1 (321-326, purple), and β6–2 (431-435, black); **B**) and **C**) Details of the key interactions detected in the equilibrated Molecular Dynamics snapshots of **2f** (**B**) and **2e** (**C**) in complex with MT 14DM; **D**) MM/PBSA values of the enthalpy ($\Delta E_{vdW} + \Delta E_{ele}$ and $\Delta G_{PB} + \Delta G_{NP}$), entropy (-T$\Delta$S), and free energy of binding (ΔG_{bind}) for compounds **2e** and **2f**; **E**) Per residue binding free energy decomposition ($\Delta H_{bind,res}$) for MT 14DM protein in complex.

unfavourable net electrostatic contribution to the binding (36.02 kcal/mol for **2e** and 36.45 kcal/mol for **2f**). Furthermore, as expected for a typical protein/small inhibitor system, also the calculated changes in solute entropy, -TΔS, tend to oppose the binding with the 14DM (12.48 kcal/mol for **2e** and 12.41 kcal/mol for **2f**). Despite the entropy contribution and the somewhat larger unfavourable desolvation energy, in harmony with their larger molecular polarity, the enhanced electrostatic and van der Waals contribution make

these molecules tighter binders. In fact, the resulted ΔG_{bind} values are -7.21 kcal/mol for **2e** and -7.48A kcal/mol for **2f**, respectively, proving a significant good binding affinity with respect of 14DM in agreement with their inhibition activity testified by their corresponding MIC.

A quantification of the single contribution of each 14DM residue to inhibitors binding was further carried out through a per-residue binding free energy decomposition (PRBFED) of the enthalpic term ($\Delta H_{bind,res}$) of the binding free energy,

10

as shown in Fig. **3E** and this analysis allowed us to better discriminate the slight difference in the 14DM binding affinity of **2e** and **2f**. The PRBFED analysis confirmed that the network of favourable enthalpic interactions is substantially afforded by the above mentioned 14DM residues. In particular, the network of hydrophobic interactions involving the common 2,6-dichlorophenyl ring and the protein cavity generated by residues A73, A75, F78, and L321 considerably concurs in stabilizing 14DM /inhibitor binding, with an overall contribution of -5.36 kcal/mol for **2e** and -5.33 kcal/mol for **2f**. Contextually, the π-π interaction with the same molecular region and the side chains of Y76 produce a favourable contribution of -2.50 kcal/mol for **2e** and -2.47 kcal/mol for **2f**.

Lastly, the PRBFED further highlighted the importance of the other aromatic ring of the molecules, denoting a small preference of the 14DM to interact with the thiophene derivative **2f**. Indeed, the hydrophobic interactions with the second binding cavity (residues I82, L172, F255, A256 and V434) as well as the additional π-π interaction provided by F83 resulted lightly more stabilizing for **2f** compared to the biphenyl derivative **2e** (-9.11 kcal/mol for **2e** and -9.84 kcal/mol for **2f**).

CONCLUSION

In conclusion, this work highlights the importance of zinoconazole **2f** and some of its analogues as potential antimycobacterial drugs gifted with good antimycobacterial activity towards Mtb (*i.e.* compounds **2d** and **2e**). All the synthetized compounds were also tested for their toxicity towards mammalian cells (Vero). Interestingly, all the azole derivatives revealed a significant cytotoxic but, among them, the 4-phenyl derivatives (**2e** and **2k**) resulted to be less toxic than zinoconazole **2f**, and compound **2e** showing one of the best MIC value against Mtb of 8 μg/ml and a selectivity index of 15.

From the data obtained the importance of the presence of the imidazole ring is clear, in comparison with the triazole nucleus, for the inhibitory activity towards Mtb, and that the modulation of the aryl moiety can improve the effectiveness of the inhibition, as well as the selectivity towards mycobacterial cell target. Moreover, the relevance of the dichlorophenyl ring as a key element also for the antimycobacterial activity was confirmed. In particular the (*Z*)-1-(2-([1,1'-biphenyl]-4-yl)-2-(2-(2,6-dichlorophenyl)hydrazono)ethyl)-1H-imidazole derivative, **2e**, revealed a promising antimycobacterial property and a safe cytotoxic profile.

These evidences could be useful for the future development of new antimycobacterial derivatives targeting CYP51 with more specificity for the mycobacterial cell enzyme.

ETHICS APPROVAL AND CONSENT TO PARTICIPATE

Not applicable.

HUMAN AND ANIMAL RIGHTS

No Animals/Humans were used for studies that are base of this research.

CONSENT FOR PUBLICATION

Not applicable.

AVAILABILITY OF DATA AND MATERIALS

The authors confirm that the data supporting the findings of this study are available within the article and its supplementary materials.

CONFLICT OF INTEREST

The authors declare no conflict of interest, financial or otherwise.

REFERENCES

[1] WHO-global tuberculosis report. World Health Organization **2017**, 1-262.

[2] Yadav, D.K.; Ahmad, I.; Shukla, A.; Khan, F.; Negi, A.S.; Gupta, A. QSAR and docking studies of chalcone derivatives for antitubercular activity against M. tuberculosis H37Rv. *J. Chemometr.*, **2014**, *28*, 499-507. [http://dx.doi.org/10.1002/cem.2606]

[3] Bhat, Z.S.; Rather, M.A.; Syed, K.Y.; Ahmad, Z. α-pyrones and their hydroxylated analogs as promising scaffolds against Mycobacterium tuberculosis. *Future Med. Chem.*, **2017**, *9*(17), 2053-2067. [http://dx.doi.org/10.4155/fmc-2017-0116] [PMID: 29076769]

[4] Makarov, V.; Manina, G.; Mikusova, K.; Möllmann, U.; Ryabova, O.; Saint-Joanis, B.; Dhar, N.; Pasca, M.R.; Buroni, S.; Lucarelli, A.P.; Milano, A.; De Rossi, E.; Belanova, M.; Bobovska, A.; Dianiskova, P.; Kordulakova, J.; Sala, C.; Fullam, E.; Schneider, P.; McKinney, J.D.; Brodin, P.; Christophe, T.; Waddell, S.; Butcher, P.; Albrethsen, J.; Rosenkrands, I.; Brosch, R.; Nandi, V.; Bharath, S.; Gaonkar, S.; Shandil, R.K.; Balasubramanian, V.; Balganesh, T.; Tyagi, S.; Grosset, J.; Riccardi, G.; Cole, S.T. Benzothiazinones kill Mycobacterium tuberculosis by blocking arabinan synthesis. *Science*, **2009**, *324*(5928), 801-804. [http://dx.doi.org/10.1126/science.1171583] [PMID: 19299584]

[5] Sharma, K.; Tanwar, O.; Sharma, S.; Ali, S.; Alam, M.M.; Zaman, M.S.; Akhter, M. Structural comparison of Mtb-DHFR and h-DHFR for design, synthesis and evaluation of selective non-pteridine analogues as antitubercular agents. *Bioorg. Chem.*, **2018**, *80*, 319-333. [http://dx.doi.org/10.1016/j.bioorg.2018.04.022] [PMID: 29986181]

[6] Fioravanti, R.; Biava, M.; Porretta, G.C.; Artico, M.; Lampis, G.; Deidda, D.; Pompei, R. N-substituted 1-aryl-2(1H-imidazol-1-yl)1-ethanamines with broad spectrum *in vitro* antimycobacterial and antifungal activities. *Med. Chem. Res.*, **1997**, *7*, 87-97.

[7] Biava, M.; Fioravanti, R.; Porretta, G.C.; Sleiter, G.; Ettorre, A.; Deidda, D.; Lampis, G.; Pompei, R. New toluidine derivatives with

antimycobacterial and antifungal activities. *Med. Chem. Res.,* **1997**, *7*, 228-250.

[8]   Mamolo, M.G.; Zampieri, D.; Falagiani, V.; Vio, L.; Fermeglia, M.; Ferrone, M.; Pricl, S.; Banfi, E.; Scialino, G. Antifungal and antimycobacterial activity of new N1-[1-aryl-2-(1Himidazol-1-yl and 1H-1,2,4-triazol-1-yl)-ethylidene]-pyridine-2-carboxami-drazone derivatives: a combined experimental and computational approach. *ARKIVOC,* **2004**, *5*, 231-250.

[9]   Banfi, E.; Scialino, G.; Zampieri, D.; Mamolo, M.G.; Vio, L.; Ferrone, M.; Fermeglia, M.; Paneni, M.S.; Pricl, S. Antifungal and antimycobacterial activity of new imidazole and triazole derivatives. A combined experimental and computational approach. *J. Antimicrob. Chemother.,* **2006**, *58*(1), 76-84. [http://dx.doi.org/10.1093/jac/dkl182] [PMID: 16709593]

[10]   Zampieri, D.; Mamolo, M.G.; Vio, L.; Banfi, E.; Scialino, G.; Fermeglia, M.; Ferrone, M.; Pricl, S. Synthesis, antifungal and antimycobacterial activities of new bis-imidazole derivatives, and prediction of their binding to P450$_{(14DM)}$ by molecular docking and MM/PBSA method. *Bioorg. Med. Chem.,* **2007**, *15*(23), 7444-7458. [http://dx.doi.org/10.1016/j.bmc.2007.07.023] [PMID: 17888669]

[11]   Zampieri, D.; Mamolo, M.G.; Laurini, E.; Scialino, G.; Banfi, E.; Vio, L. Antifungal and antimycobacterial activity of 1-(3,5-diaryl-4,5-dihydro-1H-pyrazol-4-yl)-1H-imidazole derivatives. *Bioorg. Med. Chem.,* **2008**, *16*(8), 4516-4522. [http://dx.doi.org/10.1016/j.bmc.2008.02.055] [PMID: 18321714]

[12]   Zampieri, D.; Mamolo, M.G.; Laurini, E.; Scialino, G.; Banfi, E.; Vio, L. 2-aryl-3-(1H-azol-1-yl)-1H-indole derivatives: a new class of antimycobacterial compounds - conventional heating in comparison with MW-assisted synthesis. *Arch. Pharm. (Weinheim),* **2009**, *342*(12), 716-722. [http://dx.doi.org/10.1002/ardp.200900031] [PMID: 19921681]

[13]   Bellamine, A.; Mangla, A.T.; Nes, W.D.; Waterman, M.R. Characterization and catalytic properties of the sterol 14alpha-demethylase from Mycobacterium tuberculosis. *Proc. Natl. Acad. Sci. USA,* **1999**, *96*(16), 8937-8942. [http://dx.doi.org/10.1073/pnas.96.16.8937] [PMID: 10430874]

[14]   Dyer, R.L.; Ellames, G.J.; Hamill, B.J.; Manley, P.W.; Pope, A.M. Synthesis of (E)-1-(5-chlorothien-2-yl)-2-(1H-imidazol-1-yl)ethanone 2,6-dichlorophenylhydrazone hydrochloride, a novel, orally active antifungal agent. *J. Med. Chem.,* **1983**, *26*(3), 442-445. [http://dx.doi.org/10.1021/jm00357a023] [PMID: 6298430]

[15]   Ali, M.A.; Shaharyar, M.; Siddiqui, A.A. Synthesis, structural activity relationship and anti-tubercular activity of novel pyrazoline derivatives. *Eur. J. Med. Chem.,* **2007**, *42*(2), 268-275. [http://dx.doi.org/10.1016/j.ejmech.2006.08.004] [PMID: 17007966]

[16]   Ali, M.A.; Yar, M.S. Antitubercular activity of novel substituted 4,5-dihydro-1H-1-pyrazolylmethanethiones. *J. Enzyme Inhib. Med. Chem.,* **2007**, *22*(2), 183-189. [http://dx.doi.org/10.1080/14756360601072437] [PMID: 17518345]

[17]   Mullen, J.B.; Swift, P.A.; Marinyak, D.M.; Allen, S.D.; Mitchell, J.T.; Kinsolvin, C.R.; Georgiev, V.St. Studies on antifungal agents. Part 22. 3-Aryl-5[(aryloxy)alkyl]-3-[(1H-imidazol-1-yl)methyl]-2-methylisoxazolidines and related derivatives. *Helv. Chim. Acta,* **1988**, *71*, 18-32. [http://dx.doi.org/10.1002/hlca.19880710406]

[18]   Chapman, D.R.; Bauer, L. Synthesis and carbon-13 NMR spectra of cis- and trans-2-(haloaryl)-2-(1H-imidazol-1-ylmethyl)-1,3-dioxolane-4-methanols. *J. Het. Chem.,* **1990**, *27*, 2053-2061. [http://dx.doi.org/10.1002/jhet.5570270738]

[19]   Lakshmanan, B.; Mazumder, P.M.; Sasmal, D.; Ganguly, S. Synthesis, antispasmodic and antidiarrheal activities of some 1-substituted imidazole derivatives. *Acta Pharm.,* **2011**, *61*(2), 227-236. [http://dx.doi.org/10.2478/v10007-011-0014-6] [PMID: 21684849]

[20]   Astleford, B.A.; Goe, G.L.; Keay, J.G.; Scriven, E.F.V. Synthesis of 1-alkyl-1,2,4-triazoles: a new one-pot regiospecific procedure. *J. Org. Chem.,* **1989**, *54*, 731-732. [http://dx.doi.org/10.1021/jo00264a048]

[21]   Roman, G.; Vlahakis, J.Z.; Vukomanovic, D.; Nakatsu, K.; Szarek, W.A. Heme oxygenase inhibition by 1-aryl-2-(1h-imidazol-1-yl/1h-1,2,4-triazol-1-yl)ethanones and their derivatives. *ChemMedChem,* **2010**, *5*(9), 1541-1555. [http://dx.doi.org/10.1002/cmdc.201000120] [PMID: 20652928]

[22]   Xu, Liang-zhong; Zhang, Shu-sheng; Gao, Hong-rong; Jiao, Kui. Studies on synthesis and biological activities of novel triazole compounds containing pyrimidine or N,N-dialkyldithiocarbamate ring. *Chem. Res. In China Univ,* **2003**, *19*, 437-441.

[23]   Fellner, P.J.; Hamill, B.J.; Manley, P.W. G.D. Searle & Co. *US Patent 4351948,* **1982**.

[24]   Palomino, J.C.; Martin, A.; Camacho, M.; Guerra, H.; Swings, J.; Portaels, F. Resazurin microtiter assay plate: simple and inexpensive method for detection of drug resistance in Mycobacterium tuberculosis. *Antimicrob. Agents Chemother.,* **2002**, *46*(8), 2720-2722. [http://dx.doi.org/10.1128/AAC.46.8.2720-2722.2002] [PMID: 12121966]

[25]   Taneja, N.K.; Tyagi, J.S. Resazurin reduction assays for screening of anti-tubercular compounds against dormant and actively growing Mycobacterium tuberculosis, Mycobacterium bovis BCG and Mycobacterium smegmatis. *J. Antimicrob. Chemother.,* **2007**, *60*(2), 288-293. [http://dx.doi.org/10.1093/jac/dkm207] [PMID: 17586560]

[26]   Zampieri, D.; Mamolo, M.G.; Laurini, E.; Fermeglia, M.; Posocco, P.; Pricl, S.; Banfi, E.; Scialino, G.; Vio, L. Antimycobacterial activity of new 3,5-disubstituted 1,3,4-oxadiazol-2(3H)-one derivatives. Molecular modeling investigations. *Bioorg. Med. Chem.,* **2009**, *17*(13), 4693-4707. [http://dx.doi.org/10.1016/j.bmc.2009.04.055] [PMID: 19467603]

[27]   Morris, G.M.; Huey, R.; Lindstrom, W.; Sanner, M.F.; Belew, R.K.; Goodsell, D.S.; Olson, A.J. AutoDock4 and AutoDock-Tools4: Automated docking with selective receptor flexibility. *J. Comput. Chem.,* **2009**, *30*(16), 2785-2791. [http://dx.doi.org/10.1002/jcc.21256] [PMID: 19399780]

[28]   Mehler, E.L.; Solmajer, T. Electrostatic effects in proteins: comparison of dielectric and charge models. *Protein Eng.,* **1991**, *4*(8), 903-910. [http://dx.doi.org/10.1093/protein/4.8.903] [PMID: 1667878]

[29]   a) Onufriev, A.; Bashford, D; Case, D.A. Modification of the Generalized Born Model Suitable for Macromolecules. *J. Phys. Chem.,* **2000**, *104*, 3712-3720.b) Feig, M.; Onufriev, A.; Lee, M.S.; Im, W.; Case, D.A.; Brooks, C.L., III Performance comparison of generalized born and Poisson methods in the calculation of electrostatic solvation energies for protein structures. *J. Comput. Chem.,* **2004**, *25*(2), 265-284. [http://dx.doi.org/10.1002/jcc.10378] [PMID: 14648625]

[30]   Case, D.A.; Darden, T.A.; Cheatham, T.E., III; Babin, V.; Berryman, J.; Betz, R.M.; Cai, Q.; Cerutti, D.S.; Duke, R.E.; Gohlke, H.; Goetz, A.W.; Gusarov, S.; Homeyer, N.; Janowski, P.; Kaus, J.; Kolossváry, I.; Kovalenko, A.; Lee, T.S.; LeGrand, S.; Luchko, T.; Luo, R.; Madej, B.; Merz, K.M.; Paesani, F.; Roe, D.R.; Roitberg, A.; Sagui, C.; Salomon-Ferrer, R.; Seabra, G.; Simmerling, C.L.; Smith, W.; Swails, J.; Walker, R.C.; Wang, J.; Wolf, R.M.; Wu, X.; Kollman, P.A. *AMBER 14*; University of California: San Francisco, **2012**.

[31]   Jorgensen, W.L.; Chandrasekhar, J.; Madura, J.D.; Impey, R.W.; Klein, M.L. Comparison of simple potential functions for simulating liquid water. *J. Chem. Phys.,* **1983**, *79*, 926-935. [http://dx.doi.org/10.1063/1.445869]

[32]   Ryckaert, J.P.; Ciccotti, G.; Berendsen, H.J.C. Numerical integration of the cartesian equations of motion of a system with constraints: molecular dynamics of n-alkanes. *Comput. Phys.,* **1977**, *23*, 327-341. [http://dx.doi.org/10.1016/0021-9991(77)90098-5]

[33]   Toukmaji, A.; Sagui, C.; Board, J.; Darden, T. Efficient particle-mesh Ewald based approach to fixed and induced dipolar interactions. *J. Chem. Phys.,* **2000**, *113*, 10913-10927. [http://dx.doi.org/10.1063/1.1324708]

[34]   Briguglio, I.; Loddo, R.; Laurini, E.; Fermeglia, M.; Piras, S.; Corona, P.; Giunchedi, P.; Gavini, E.; Sanna, G.; Giliberti, G.; Ibba, C.; Farci, P.; La Colla, P.; Pricl, S.; Carta, A. Synthesis, cytotoxicity and antiviral evaluation of new series of imidazo[4,5-g]quinoline and pyrido[2,3-g]quinoxalinone derivatives. *Eur. J. Med. Chem.,* **2015**, *105*, 63-79. [http://dx.doi.org/10.1016/j.ejmech.2015.10.002] [PMID: 26479028]

[35]   Carta, A.; Briguglio, I.; Piras, S.; Corona, P.; Ibba, R.; Laurini, E.; Fermeglia, M.; Pricl, S.; Desideri, N.; Atzori, E.M.; La Colla, P.; Collu, G.; Delogu, I.; Loddo, R. A combined in silico/in vitro approach unveils common molecular requirements for efficient BVDV RdRp binding of linear aromatic N-polycyclic systems. *Eur. J. Med. Chem.,* **2016**, *117*, 321-334. [http://dx.doi.org/10.1016/j.ejmech.2016.03.080] [PMID: 27161176]

[36]   Zampieri, D.; Vio, L.; Fermeglia, M.; Pricl, S.; Wünsch, B.; Schepmann, D.; Romano, M.; Mamolo, M.G.; Laurini, E. Com-

[37]   Wilson, E.B.; Decius, J.C.; Cross, P.C. *Molecular Vibrations*; McGraw-Hill: New York, **1995**.

[38]   Hartkoorn, R.C.; Chandler, B.; Owen, A.; Ward, S.A.; Bertel Squire, S.; Back, D.J.; Khoo, S.H. Differential drug susceptibility of intracellular and extracellular tuberculosis, and the impact of P-glycoprotein. *Tuberculosis (Edinb.),* **2007**, *87*(3), 248-255. [http://dx.doi.org/10.1016/j.tube.2006.12.001] [PMID: 17258938]

[39]   Podust, L.M.; Poulos, T.L.; Waterman, M.R. Crystal structure of cytochrome P450 14alpha -sterol demethylase (CYP51) from Mycobacterium tuberculosis in complex with azole inhibitors. *Proc. Natl. Acad. Sci. USA,* **2001**, *98*(6), 3068-3073. [http://dx.doi.org/10.1073/pnas.061562898] [PMID: 11248033]

[40]   Yadav, D.K.; Khan, F.; Negi, A.S. Pharmacophore modeling, molecular docking, QSAR, and in silico ADMET studies of gallic acid derivatives for immunomodulatory activity. *J. Mol. Model.,* **2012**, *18*(6), 2513-2525. [http://dx.doi.org/10.1007/s00894-011-1265-3] [PMID: 22038459]

[41]   Yadav, D.K.; Kalani, K.; Khan, F.; Srivastava, S.K. QSAR and docking based semi-synthesis and *in vitro* evaluation of 18 β-glycyrrhetinic acid derivatives against human lung cancer cell line A-549. *Med. Chem.,* **2013**, *9*(8), 1073-1084. [http://dx.doi.org/10.2174/1573406411309080009] [PMID: 23675978]

[42]   Yadav, D.K.; Khan, F. QSAR, docking and ADMET studies of camptothecin derivatives as inhibitors of DNA topoisomerase-I. *J. Chemom.,* **2013**, *27*, 21-33.

[43]   Yadav, D.K.; Dhawan, S.; Chauhan, A.; Qidwai, T.; Sharma, P.; Bhakuni, R.S.; Dhawan, O.P.; Khan, F. QSAR and docking based semi-synthesis and *in vivo* evaluation of artemisinin derivatives for antimalarial activity. *Curr. Drug Targets,* **2014**, *15*(8), 753-761. [http://dx.doi.org/10.2174/1389450115666140630102711] [PMID: 24975562]

[44]   Yadav, D.K.; Kalani, K.; Singh, A.K.; Khan, F.; Srivastava, S.K.; Pant, A.B. Design, synthesis and *in vitro* evaluation of 18β-glycyrrhetinic acid derivatives for anticancer activity against human breast cancer cell line MCF-7. *Curr. Med. Chem.,* **2014**, *21*(9), 1160-1170. [http://dx.doi.org/10.2174/09298673113206660330] [PMID: 24180274]

[45]   Raag, R.; Li, H.; Jones, B.C.; Poulos, T.L. Inhibitor-induced conformational change in cytochrome P-450CAM. *Biochemistry,* **1993**, *32*(17), 4571-4578. [http://dx.doi.org/10.1021/bi00068a013] [PMID: 8485133]